Rotary Kiln Monitoring with Shell Temperature Visualization and Process Analytics

Lee Rippon the University of British Columbia and Spartan Controls, **Barry Hirtz** Cool Cameras, **Carl Sheehan** Spartan Controls, **Travis Reinheimer** Canfor Pulp, **Cilius van der Merwe** Canfor Pulp, **Philip Loewen** the University of British Columbia, and **Bhushan Gopaluni** the University of British Columbia

ABSTRACT

Rotary kilns are energy-intensive unit operations that perform important functions in a variety of industrial processes including cement production, pyrometallurgy, and kraft pulping. As a critical reactor in the recovery circuit of kraft pulp mills it is essential for rotary lime kiln operation to be optimized to meet economic and environmental objectives. Rotary lime kilns are increasingly outfitted with advanced sensing technology, such as thermal cameras, to provide additional insights into operation, maintenance, and process troubleshooting. Maximizing the value extracted from this additional data requires operation-specific strategies towards data collection, processing, and visualization. In this work we describe a novel strategy for rotary kiln monitoring that combines traditional process analytics with interactive visualization of large quantities of kiln shell temperature data. The proposed strategy was specifically developed to support investigation of ring formation but ultimately it has proven to be a valuable resource for monitoring and managing rotary kiln operations. This paper describes our interactive visualization strategy, demonstrates how it can be enhanced by process analytics to investigate ring formation with industrial data, and provides open-source resources for interested users.

INTRODUCTION

Rotary kilns are large-scale cylindrical vessels that consist of an inclined steel shell that is lined with refractory bricks, supported on rollers, and rotated by a drive gear. Industrial rotary kilns are expensive, energy-intensive vessels that serve as key unit operations in cement production, pyrometallurgy, and kraft pulping. The high energy intensity and important role of rotary kilns creates a strong emphasis on process monitoring and preventative maintenance to ensure safe operation and meet both economic and environmental objectives [1].

Advanced sensor technology is increasingly deployed in chemical process industries to address maintenance and operations challenges. This is exemplified by the increased adoption of infrared thermal cameras for the monitoring and control of rotary kilns [2]. Infrared thermal cameras can be used to measure shell temperatures which can provide valuable insights for safe and efficient rotary kiln operation. Identifying shell hot spots can prevent expensive damage to the refractory and the shell. Moreover, shell temperatures can provide indications of fouling, such as ring formation, which can result in unplanned shutdowns [3]. Although many kilns have deployed thermal cameras, the extent to which they are utilized is often far from optimal. To facilitate extraction and communication of process insights, engineers and operators must be able to interact with large quantities of thermal camera data in a user-friendly and visually intuitive manner. Ultimately, the objective of this work is to empower operators and engineers to improve the production efficiency of rotary kilns through enhanced process monitoring that enriches the value extracted from existing thermal camera applications.

This paper provides rotary kiln operators, engineers, and researchers with a novel strategy for monitoring kiln operations and extracting knowledge from historical data. The proposed approach enables intuitive visualization of large quantities of kiln shell temperature (KST) data. By including user-friendly interactive features, KST profiles from multiple kilns can be visualized alongside relevant process variables (PVs) at varying timescales (i.e., hours to years) with options for statistical process control (SPC) limits and rules. Originally, this visualization strategy was developed to visualize the formation of rings which can grow and decay on a timescale between days and months. However, upon receiving positive feedback and increased attention from industry, it has become apparent that this visualization strategy is also useful for more general operations management, optimization, and troubleshooting. To demonstrate the proposed visualization strategy an industrial case study from a lime kiln in a kraft pulp mill is presented. Finally, for the rotary kiln professionals who are interested in applying this visualization to their own data an instructive tutorial is provided with implementation resources, open-source code, and synthetic kiln data.

BACKGROUND

The process monitoring techniques presented in this work are generally applicable to rotary kilns that are equipped with sensors that provide real-time KST measurements along the length of the kiln (e.g., infrared thermal cameras). However, to provide context and better demonstrate the proposed strategy we will focus on a rotary lime kiln that is an integral part of the recovery circuit in a kraft pulp mill. The recovery circuit serves important economic and environmental roles by reconstituting white liquor after it is spent in the digester to delignify wood chips. Specifically, white liquor and calcium carbonate (i.e., lime mud) are produced by calcium oxide (i.e., lime) causticizing sodium carbonate in the causticizing plant. The lime kiln regenerates calcium oxide from calcium carbonate through the endothermic calcination reaction,

$$\mathrm{CaCO_3}(s) \rightarrow \mathrm{CaO}(s) + \mathrm{CO_2}(g),$$

which requires approximately 3 MJ of energy to produce 1 kg of pure CaO at 900°C [4, 5].

Rotary lime kilns can be over 100 m long with an inner diameter of 4 m. The top of the inclined kiln (i.e., the feed end) is where lime mud enters the kiln and carbon dioxide gas is exhausted. Lime has a residence time of roughly 2 to 3 hours in the kiln depending on the slope of the kiln (approximately 2º) and the speed of rotation (roughly 1 rpm). As Figure 1 illustrates, the calcium carbonate mud enters the kiln and begins drying into a powder before it is pre-heated from approximately 80°C to about 870°C, at which point calcination begins. Calcium oxide nodules with approximately 1-5% residual $CaCO_3$ exit from the bottom of the kiln (i.e., the firing end) where the burner is located. Chains are often hung in the drying section of the kiln to provide a heat exchange surface and compensate for lower feed end gas temperatures [5-7]. The yellow field in Figure 1 illustrates a thermal camera measuring the shell temperatures along the length of the kiln.

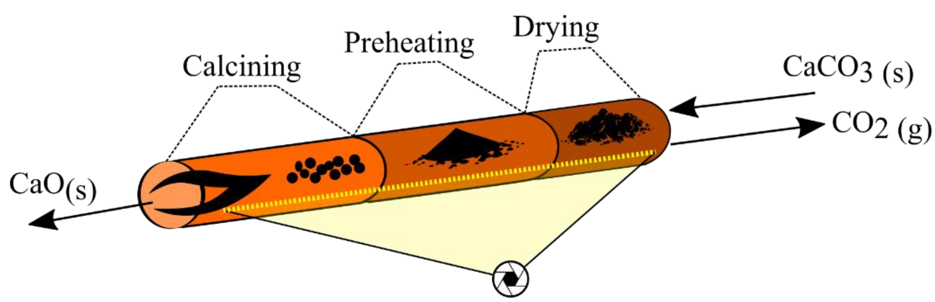

Figure 1: Simplified illustration of a rotary lime kiln with a thermal camera measuring the shell temperature.

Traditionally, temperature sensors at the firing end of the kiln have been used for fuel control while feed end temperature sensors have been used for induced draft fan control [8]. As industrial thermal imaging technology has matured it has achieved substantial performance improvements while becoming significantly more affordable. Consequently, thermal imaging tools (e.g., infrared cameras) have gained increased interest for monitoring and advanced control of rotary kiln operations [2]. This work primarily focuses on novel applications of large quantities of shell temperature measurements to improve monitoring and operation of rotary lime kilns. Shell temperature profiles can be measured with a one-dimensional line scanner that has a rotating head calibrated to the rotation speed of the kiln. Alternatively, stationary two-dimensional thermal cameras can be configured to measure shell temperatures in various ways including measurement areas and profile lines, such as those shown in Figure 2 [9].

Although many operations measure shell temperatures in real-time, there is often significant value in the KST data that goes unappreciated and in unfortunate circumstances, becomes permanently discarded. Broad applications of real-time KST measurements include process monitoring, fault detection and diagnosis, abnormal situation

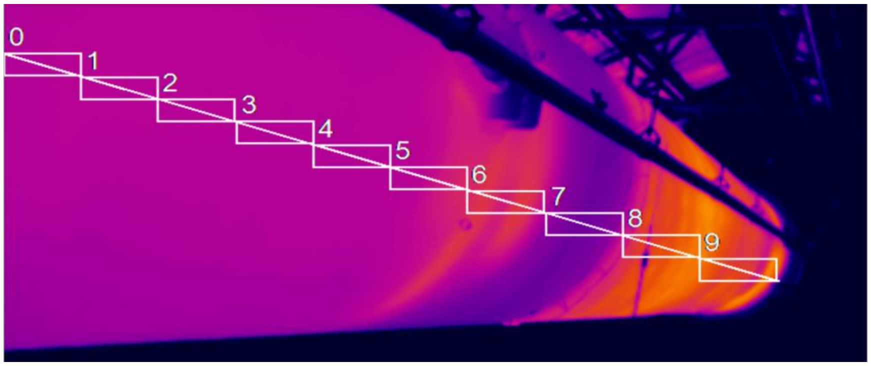

Figure 2: A stationary two-dimensional infrared thermal camera measures shell temperatures along a rotary lime kiln [9]. The thermal camera can be configured to extract shell temperatures along the continuous diagonal profile line or to average the temperatures within the discrete rectangular measurement areas.

management, kiln modelling, and advanced process control. Specifically, KST data can prevent catastrophic events by triggering safety procedures when shell hot spots surpass preset temperature limits. Real-time shell temperatures can help mitigate unnecessary refractory wear and quantify the shell heat loss [10]. Shell temperatures can provide valuable context to help evaluate the efficiency of start-ups. The use of shell temperatures to infer the state of fouling inside the kiln is of significant value to kilns that experience frequent problems with ring growth [2, 11, 12].

Ring formation is a type of kiln fouling that has been described in the literature as the most troublesome problem for lime kiln operation [4]. The left side of Figure 3 demonstrates a related type of kiln fouling in the chain section of the kiln, commonly referred to as soda balls, which are sometimes observed in kilns with frequent ring problems. Soda balls are suspected to be caused by alkali (i.e., sodium hydroxide) volatilizing in the hot end of the kiln and condensing in the chain section. Rings form when lime mud or product lime particles adhere to the refractory wall. The right side of Figure 3 demonstrates two distinct ring growth events, both of which resulted in lost production time. The ring orifice can reduce lime production, costing over $50,000 per day in purchased lime rock. In particularly bad cases the ring can cause damage to either the shell or the refractory lining which can result in repairs and lost production that cost over $3 million per event [13].

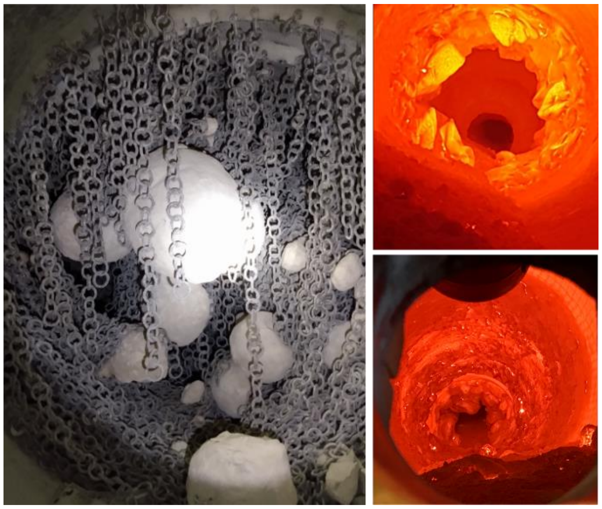

Figure 3: **Left:** fouling in the chain section of a kiln. These ‘soda balls’ are suspected to be caused by volatilized alkali condensing in the chain section [13]. **Right:** Two separate cases of ring formation that resulted in lost production time. The image on the bottom right shows the burner and the refractory bricks.

Rings can be reduced by thermal cycling to cause stress fractures, adding water to the kiln (i.e., slaking) to dissolve and soften the ring, shooting the ring with an industrial 8-gauge shotgun, and blasting with high pressure carbon dioxide (i.e., cardox) [13]. For complete removal it is often necessary to shut down the kiln and wait for it to cool enough for someone to enter the kiln and use a pneumatic jack hammer to physically remove the ring [14]. As rings age they can harden through recarbonation, becoming more difficult and costly to remove [15]. If they continue to grow unnoticed the likelihood that they will cause significant damage to the kiln increases. Therefore, early detection of rings through effective kiln monitoring is paramount for minimizing their impact on operations and identifying process conditions that lead to ring formation. In what follows, we discuss strategies to increase the value extracted from large quantities of KST data through interactive visualization and process analytics.

MONITORING WITH INTERACTIVE VISUALIZATION AND PROCESS ANALYTICS

Rings can form at significantly different rates, with noticeable deposits accumulating quickly over a matter of days or gradually over a matter of months. This large variation in the timescale of formation creates challenges for detecting ring growth that have not been addressed by conventional shell temperature visualization methods [9, 16]. Although the two-dimensional thermal camera image shown in Figure 2 provides valuable real-time insights for operators, it offers limited insights into the evolution of ring formation over long periods of time. Commercial software can be used to reconstruct an image of the kiln surface over a full rotation with an axis that shows the temperature variability over the circumference of the kiln as demonstrated by Figure 4. Kiln shell scans like the one shown in Figure 4 can provide insights into the uniformity of the refractory and the fouling along the inner circumference of the shell. However, since these shell scans represent a single kiln rotation, they do not provide insights into the dynamics of ring formation. Variations in the KST profile over time could be observed by comparing shell scans from different periods but this would be cumbersome and ineffective.

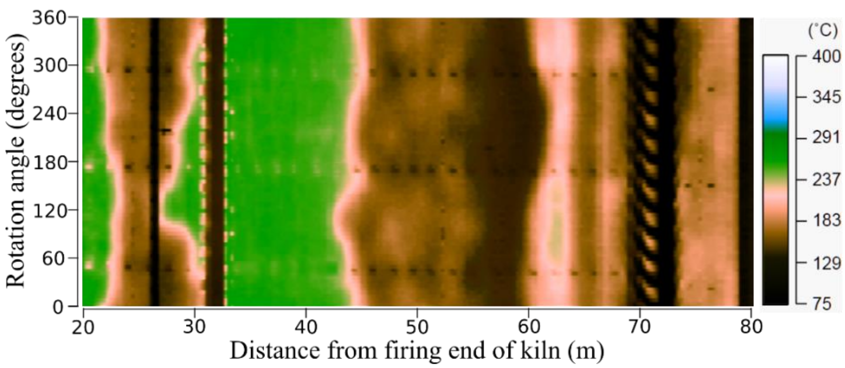

Figure 4: A kiln shell scan that shows axial KST variations along the x-axis and circumferential KST variations along the y-axis. These shell scan visualizations are often produced by commercial software combined with a one-dimensional line scanner with a rotating head calibrated to the rotation speed of the kiln.

To detect rings the KST profile needs to be visualized over varying periods of time. A common approach in industry is to overlay KST profiles taken from different periods of interest as demonstrated by the three KST profiles shown in Figure 5. The KST profiles in Figure 5 are taken from a profile line like the diagonal profile line in Figure 2 except these measurements are from the firing end of the kiln. This firing end profile line is from a single camera, and it contains roughly 330 measurements, collected every five seconds, and averaged between 15:00-16:00 on the dates shown in the legend. Between 2021-08-05 and 2021-08-15 there was a substantial drop in the overall KST profile. By 2021-08-25 most of the firing end profile had recovered except for between ten to fifteen meters from the firing end where there is notable offset that potentially indicates ring growth. While this approach to visualizing shell temperatures does provide some insights into KST profile changes over time it is still significantly limited. If too few profiles are overlayed, it is uninformative; if too many profiles are overlayed, it is incomprehensible.

To intuitively visualize large quantities of KST profiles in a user-friendly manner we propose the novel visualization strategy presented in Figure 6. This spatiotemporal heatmap shows axial shell temperature variations along the y-axis and continuous temporal shell temperature variations along the x-axis. The y-axis temperatures from Figure 5

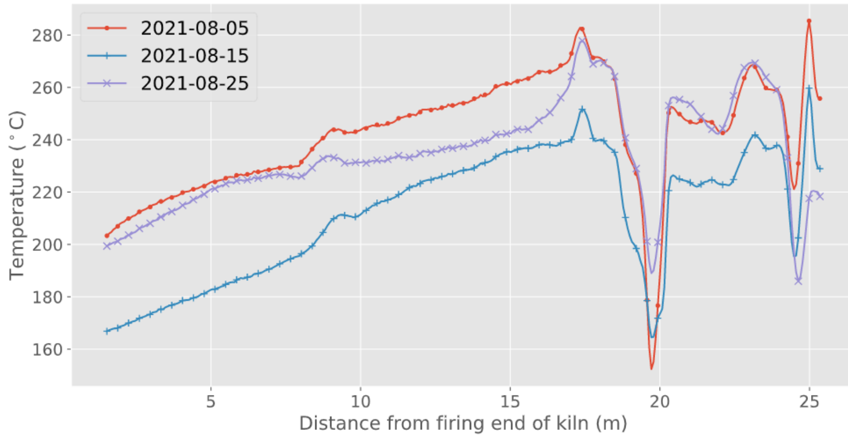

Figure 5: Comparing shell temperature profiles from the firing end of the kiln in ten-day intervals. On each day the KST measurements are averaged between 15:00-16:00. The drop in temperature approximately 20 meters from the firing end of the kiln is due to external bracing.

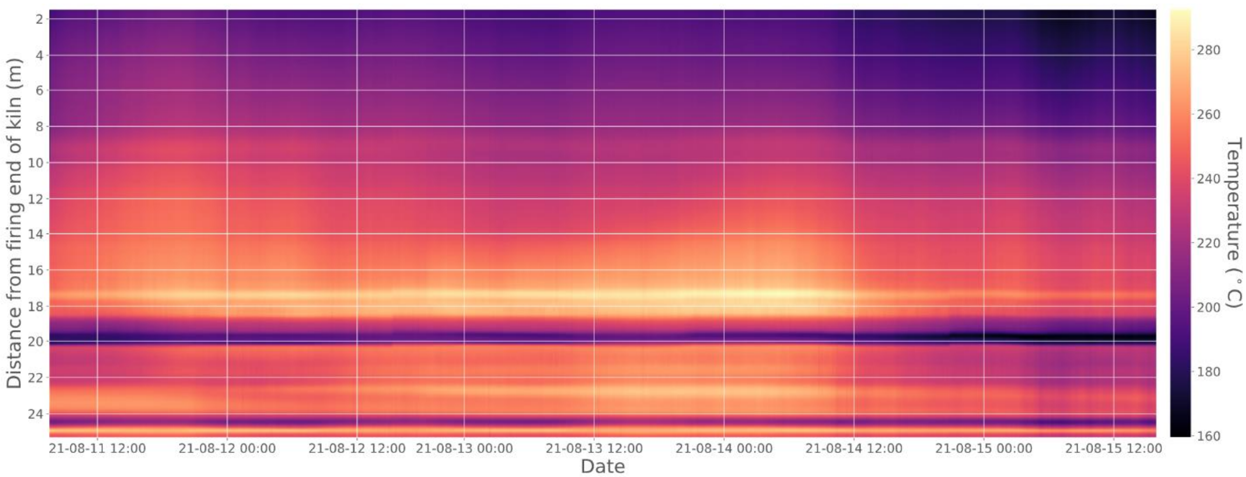

Figure 6: Spatiotemporal heatmap of KST profiles in the four days leading up to the cold profile on 2021-08-15 from Figure 5. By continuously observing KST variations we can easily identify 2021-08-14 at 12:00 as the time that the KST profiles started significantly dropping.

are embedded as the uniform, sequential colormap on the right side of Figure 6. Embedding the temperatures as colors enables a clear, intuitive visualization of large quantities of KST data. Although minor variations in temperature might not appear as clearly as they do in Figure 5, there is a substantial benefit to being able to continuously monitor these variations over time. Moreover, the contrast in color between small temperature variations can be increased by omitting the external bracing. The data in Figure 6 is the same firing end profile line data from Figure 5 except Figure 6 shows the four days leading up to the 2021-08-15 cold kiln profile which show the temperature profile began to drop off significant at approximately 12:00 on 2021-08-14. Precisely identifying the onset of these changes is critical for kiln monitoring.

To implement this visualization strategy interested readers are referred to our original publication which outlined a detailed procedure to convert KST data collected from rectangular measurement areas into the spatiotemporal heatmap. Previous work also demonstrates how the spatiotemporal heatmap can be complemented by interactive features to enable visualization of rings over varying timescales and in the context of relevant process variables (PVs) [9]. Instead of reiterating this information, this paper will demonstrate extended functionality of the interactive visualization strategy and show how process analytics can be used to complement the data visualization and improve kiln monitoring.

Interactive Visualization of Large Quantities of Shell Temperature Data

Before the extended functionality of the interactive KST visualization tool is introduced the preliminary steps are briefly reviewed. It is important to note that the proposed approach to visualizing KST data can be accomplished with various thermal measurement technologies, i.e., single-point line scanners or two-dimensional infrared cameras, regardless of whether the data is collected as a continuous profile line or as unequally spaced rectangular measurement areas. The only requirement is that relatively frequent numeric KST data is available over known axial positions along the kiln such that a matrix of KST measurements, $\boldsymbol{T}(\boldsymbol{x}, \boldsymbol{t})$, can be constructed where the rows $\boldsymbol{x} = [x_1, x_2, \ldots, x_n]$ represent the axial position of measurements and the columns $\boldsymbol{t} = [t_1, t_2, \ldots, t_\tau]$ represent the sampling times. If the axial positions are not equally spaced, piecewise linear interpolation can be performed to up-sample each KST profile. Interactive parameters for the start date and window size can be included to visualize KST profiles at varying time scales. Moreover, users can select from a list of relevant PVs to plot below the heatmap which helps add important context to the shell temperatures. Figure 7 demonstrates the heatmap, PV plot, and interactive dashboard created to monitor large quantities of shell temperatures data.

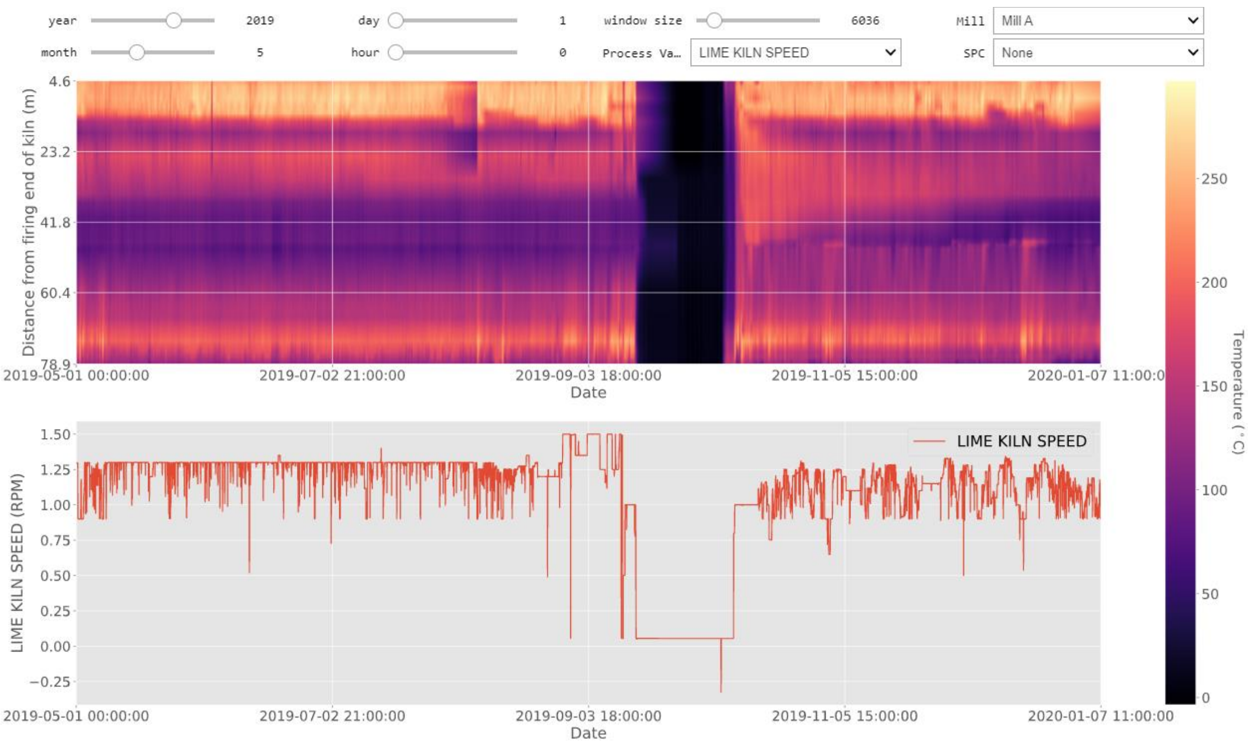

Figure 7: Improved monitoring and investigation of KST profiles with spatiotemporal heatmaps, complementary PVs, and interactive features. Roughly eight months of hourly averaged KST data is visualized along with the lime kiln speed. Users can specify the start date and the window size (in hours) of the data presented. Relevant PVs (e.g., lime kiln speed) can be selected from a drop-down menu.

Figure 7 also illustrates two additional interactive features that were recently added for extended functionality. Shortly after this approach to visualizing the KST data was first developed it gained interest from other mills that have underutilized real-time KST measurements. It is not uncommon for kraft pulp producers to operate more than one kiln. To effectively analyze datasets from multiple kilns the visualization function was enhanced such that users can select from a list of different mills (or different kilns in the same mill). This feature is demonstrated by Figure 8 which presents the KST visualization if "Mill B" is selected. When a new mill is selected the interactive features automatically update such that only the dates and PVs that are available for that mill are presented. The y-axis labels update to reflect the position of the axial measurements on the new kiln. If a new PV is selected the axis labels and the legend also update automatically. The other interactive feature in Figure 7 that was not introduced in prior work is the statistical process control (SPC) option which is explained in the following section.

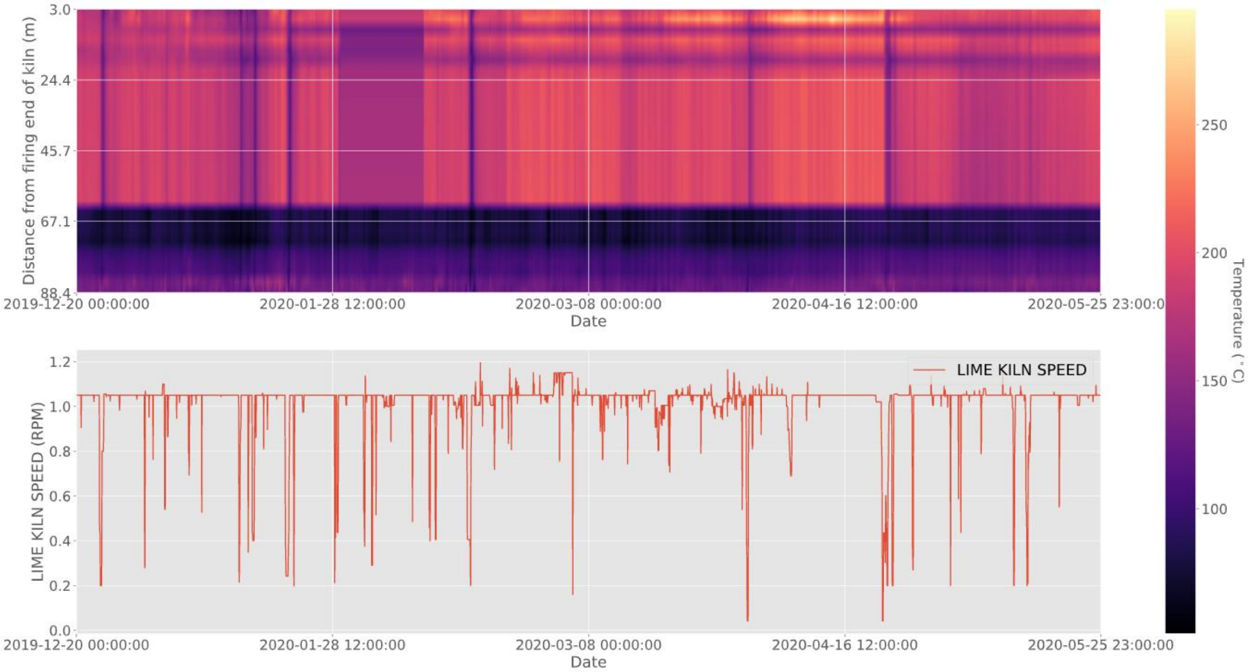

Figure 8: Visualizing approximately five months of hourly-averaged KST data from a different mill. Note the overlap in dates with Figure 7 and the clear differences between the two heatmaps. The lime kiln speed plotted below adds context to the dark vertical bands in the heatmap, i.e., the kiln was briefly shutdown. Also note the changes in the KST measurement positions and the slower rotation speed of the kiln.

Enhanced Monitoring with Process Analytics

Process data analytics have become increasingly important for industrial processes in a competitive environment that is accelerating towards data-driven intelligent manufacturing systems. Recent advances in smart process analytics combine data characteristics with expert domain knowledge for automated predictive modelling [17]. Traditional process analytics can be traced back to the use of logistic regression to describe autocatalytic chemical reactions in the early 19th century and the development of Shewhart control charts in the 1920s [18]. In this work we integrate straightforward traditional SPC concepts into our kiln monitoring approach to complement the shell temperature visualization. Specifically, the SPC feature shown in Figure 7 allows users to select options that overlay a control chart onto the PV plot below the KST heatmap. A comprehensive introduction to control charts is beyond the scope of this paper so interested readers are referred to the work from TAPPI PEERS 2019 that served as motivation for this additional feature [19].

In essence, control charts are created by calculating statistical properties (e.g., mean and standard deviation) of a key product quality variable and plotting them with the variable to identify and reduce sources of variation. The mean of the data, μ, is at the center of the sigma limits, where the one-sigma limits are offset by one standard deviation, σ, i.e., $\mu \pm \sigma$. The two-sigma limits and three-sigma limits are given by $\mu \pm 2\sigma$ and $\mu \pm 3\sigma$, respectively. The three-sigma limits are also referred to as the upper and lower control limits and the first of the five basic rules for taking action is that any values that exceed the three-sigma limits are flagged as a source of special cause variation. The remaining four rules are as follows: ii) two or more sequential values beyond the two-sigma limits, iii) four out of five consecutive values between one-sigma and two-sigma limits, iv) seven or more consecutive values on one side of the mean, and v) seven or more consecutive points trending in one direction. Special cause variation is described as an irregular type of variation that should be eliminated through investigation of upstream influences [19].

To improve monitoring and investigation of sources of variation the control chart limits and the rules for identifying special cause variation are integrated into the monitoring and KST visualization tool. Since the five basic rules were intended for product quality variables, they are not necessarily suitable as-is for every PV. Nevertheless, as heuristics they can be customized and reinterpreted to accommodate unique PVs such as the mud filter vacuum pressure which periodically exceeds the lower control limit during sheet drops. The SPC features are demonstrated in Figure 9 with a PV that represents the percentage of solids in the lime mud being fed to the kiln. Mud solids percentage is an important parameter for kiln operation because it is directly related to specific fuel consumption, i.e., less mud solids means there is more water to evaporate prior to calcining. In Figure 9 the solid black horizontal line is the mean of the displayed PV data, the green dashed lines are the one-sigma limits, the blue dot-dashed lines are the two-sigma limits, and the purple dotted lines are the three-sigma limits, i.e., the upper and lower controls limits. Four of the five basic rules are violated across this five-day period, i.e., the pink triangles violate rule one, the cyan circle violates rule two, the yellow plus symbols violate the third rule, and the green stars violate the fourth rule. A minimum of 30 samples is suggested as a heuristic to provide meaningful statistical limits [19].

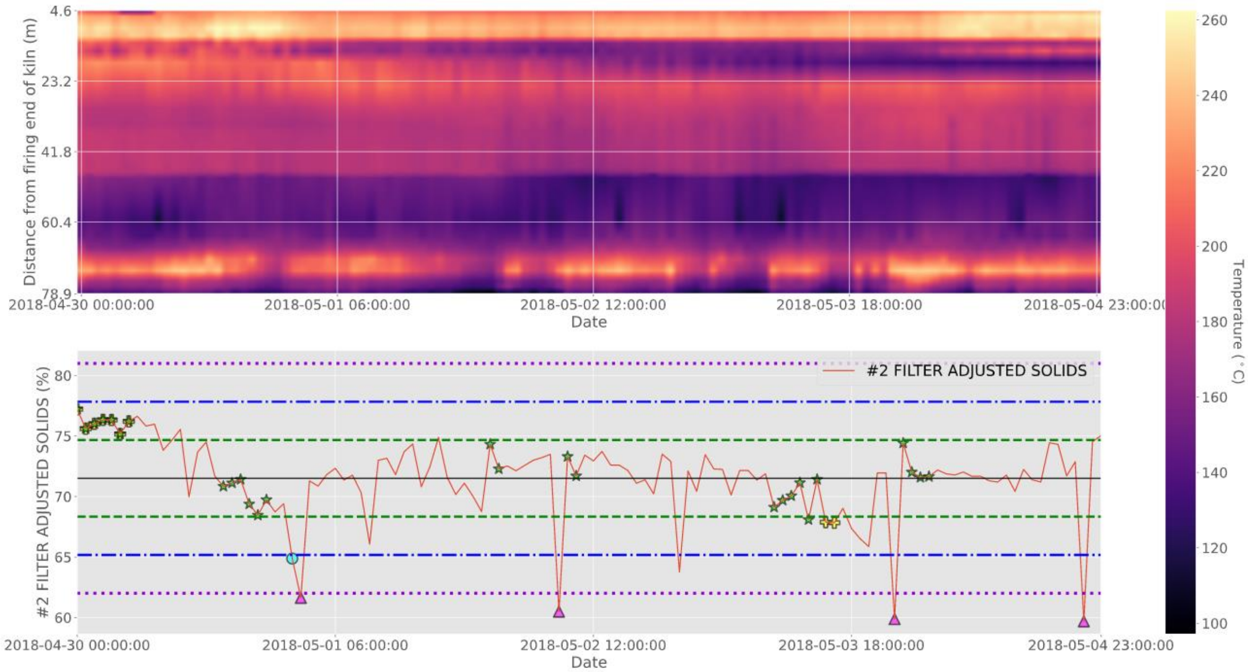

Figure 9: Demonstrating the interactive SPC feature which complements the KST visualization by flagging special cause variation in relevant PVs for further investigation. Five days of hourly averaged data are visualized. The KST heatmap shows a strong indication of ring formation at approximately 20 meters from the firing end of the kiln. The solids content of mud feeding the kiln breaks the lower control limit four times.

When large periods of data are displayed the full SPC feature can become crowded so there are options for removing rules and displaying only specific limits. Figure 9 also demonstrates how the control chart complements the KST heatmap. When periods of suspected ring formation are observed on the heatmap, relevant PVs can be investigated to see if they exhibit special cause variation. The sustained drop in shell temperatures at approximately 20 meters from the firing end of the kiln coincides with multiple lower control limit violations of the solids percentage of mud being fed to the kiln. Upstream influences on mud filter performance can be investigated to identify and potentially eliminate the source of these control limit violations. Any available PVs related to shell temperature can be analyzed for control limit violations to help characterize irregular process behavior that may contribute to ring formation.

There are certainly more technically advanced methods for monitoring and fault detection that involve training and deploying machine learning models. However, there are intrinsic advantages to intuitive visualization methods that empower end-users and subject matter experts to make more informed decisions as opposed to black-box methods with outputs that are difficult for end-users to interpret, let alone trust. An instructive tutorial with synthetic kiln data, open-source code, and implementation resources is available at https://github.com/LeeRippon/KilnVisual for those interested in implementing the interactive spatiotemporal heatmap visualization on their own kiln data [20].

INDUSTRIAL CASE STUDY – ROTATIONAL ALIASING

Thus far all the data presented in this paper has been real industrial data. In this section we will describe an industrial case study of a particular kraft pulp mill with a lime kiln that is roughly 85 m long and 3 m in diameter. The shell temperature visualization method was originally developed to investigate ring formation in this lime kiln. Resources include approximately five years of hourly averaged samples from three infrared thermal cameras and thirty relevant PVs. Five years of raw thermal camera images are also available at four-hour periods. Previous work introduced a case study on this kiln that demonstrates how the interactive KST heatmap can be used to visualize ring formation at varying timescales [9]. The case study presented here describes how our novel approach to visualizing shell temperatures revealed previously unacknowledged problems with the KST data, i.e., rotational aliasing. To our knowledge this is the first time that rotational aliasing of shell temperature data on rotary kilns has been introduced.

Three thermal cameras use rectangular measurement areas to measure the shell temperature at 24 non-equispaced locations between 4 to 79 meters away from the firing end of the kiln. The objectives of the project include early onset detection of ring formation and diagnosis of potential causes. To aid our analysis a matrix of KST measurements, $\boldsymbol{T}(\boldsymbol{x}, \boldsymbol{t})$, is constructed, each profile is up sampled with piecewise linear interpolation, and the interactive shell temperature visualization tool is developed. Ongoing research involves investigating the residual between predicted and measured shell temperatures as a potential indicator of ring formation. Preliminary results from this ring indicator were inundated with large magnitude oscillatory residuals that resulted from high frequency shell temperature variations such as those shown in Figure 10.

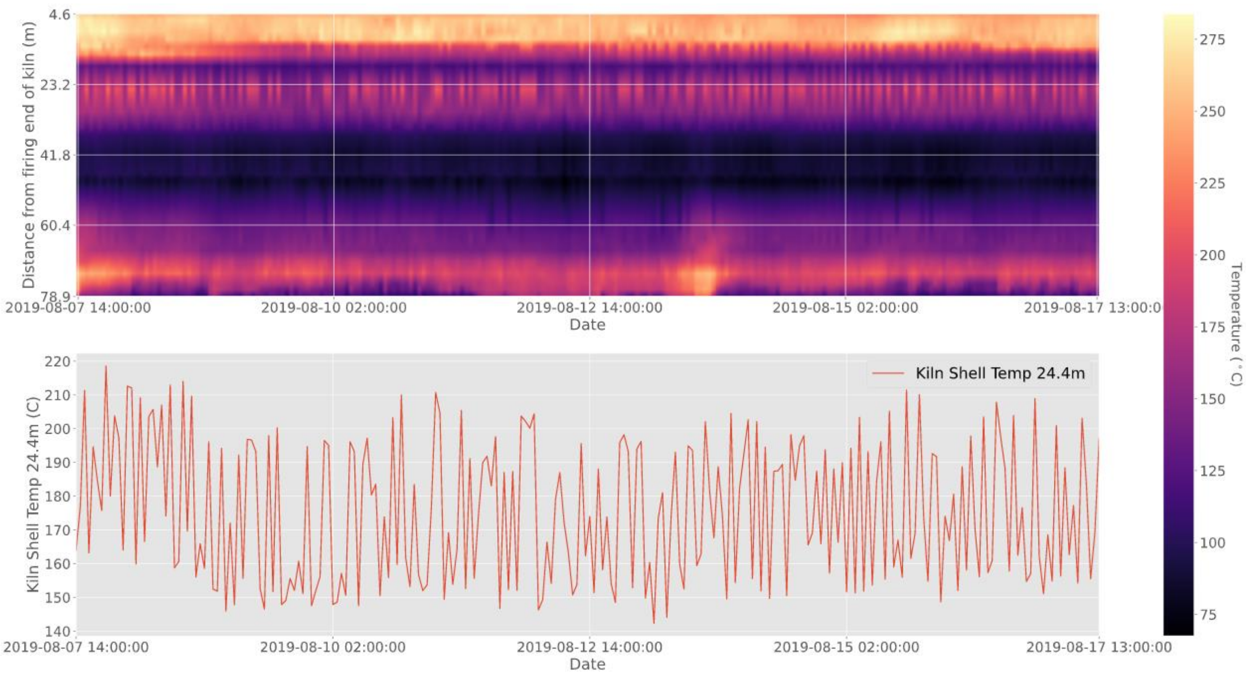

Figure 10: High frequency variations in shell temperatures measured 24.4 m from the firing end of the kiln. The heatmap gives the impression of a kiln that is undergoing drastic shell temperature changes, potentially due to a rapidly growing and decaying ring. The plot below shows the temperature changing over 50℃ in an hour.

Prior to discovering this high frequency variability, it was falsely assumed that each datapoint was roughly representative of the average temperature along the entire circumference of the shell at the given axial position. On the surface this appeared to be a reasonable assumption given the rotation speed of the kiln is just over one minute and the KST data is averaged hourly. The heatmap in Figure 10 gives the false impression of a ring rapidly growing and decaying approximately 23.2 m from the firing end of the kiln. Observing the 50℃ hourly oscillation in the plot below the heatmap led to uncertainty regarding the assumption that each hourly averaged datapoint accurately represented the average temperature over the entire shell circumference.

Further investigation into the data collection and processing revealed that the hourly averaged data is drawn from the process historian which averages from an internal database that stores KST data every minute. However, the KST data that is stored every minute is not a result of averaging even higher frequency measurements taken from the camera. Instead, the one-minute data in the process historian is collected as an instantaneous snapshot of the kiln shell that is within the measurement area. If the kiln is rotating at 1.25 rpm (as in Figure 7) then the frequency of a disturbance (e.g., fouling) at one spot along the inner circumference of the kiln is roughly 0.021 Hz. From the Nyquist-Shannon sampling theorem the minimum sampling rate required to perfectly reconstruct a signal with a frequency of 0.021 Hz is 0.042 Hz, i.e., one sample every twenty-four seconds [21]. In other words, the KST data stored in the historian did not meet the Nyquist rate of 0.042 Hz and therefore this data is insufficient for reconstructing temperature variations associated with the rotation of the kiln, e.g., fouling that is not uniformly distributed along the inner circumference of the kiln. To our knowledge this phenomenon which we refer to as rotational aliasing has not been previously described for rotary kilns. However, a similar problem is studied in paper machine control literature, i.e., separating machine direction and cross direction variations [22].

Ultimately, a new KST sampling strategy was developed such that a profile line (e.g., the diagonal line in Figure 2) is used to measure the shell temperatures and record them every five seconds. To manage the increased spatial and temporal resolutions the five-second samples are subsequently averaged into five-minute samples. The new KST profile line strategy is implemented for one of the three thermal infrared cameras, and it consists of 380 measurements located roughly 2 m to 25 m from the firing end of the kiln. Although this KST data has only been recorded for a few months a four-day heatmap is presented in Figure 6. Given that the process historian is still collecting KST data as one-minute snapshots over rectangular measurement areas it is sensible to compare the two sets of data to see if some of the high frequency noise has been attenuated.

Since there are only eight KST measurement areas from the firing end camera the comparison relies on determining which of the 380 profile line measurements best correspond to the rectangular measurement areas. Fortunately, the thermal camera software provides some assistance. The profile line data is distinguished by the x-coordinate of each pixel in the camera's field of vision. Each measurement area has a center x-coordinate that is given by the thermal camera software. For example, the center x-coordinate of the 18.3 m measurement area is 328. Therefore, profile line trends with x-coordinates between 328 ± 30 are collected and correlated with the KST data from the 18.3 m measurement area. The plot on the left side of Figure 11 shows the resulting correlation coefficient for each of the profile line positions. A maximum correlation coefficient of 0.972 is obtained at x-coordinate 325. The plot on the right side of Figure 11 shows the comparison of the measurement area data (red) with the profile line data (blue) which demonstrates the profile line strategy successfully reduced high frequency variability, especially after 2021-08-21. Although the high-frequency averaging provides a better representation of the entire kiln circumference, it can also pickup more camera obstructions creating outliers like the sharp temperature drops in Figure 11.

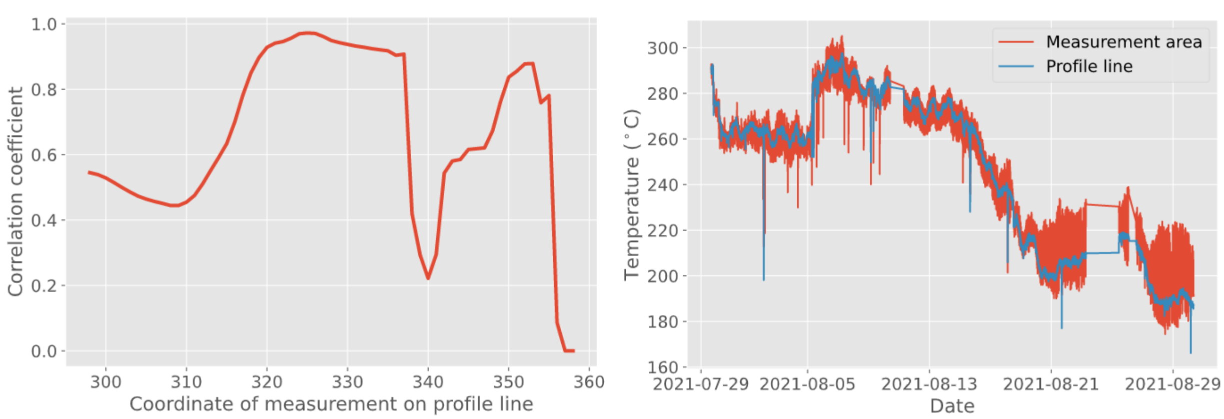

Figure 11: Comparing KST data collection methods. **Left:** the correlation coefficient between KST data from a rectangular measurement area 18.3 m from the firing end of the kiln and KST data from various profile line positions denoted by their x-coordinate along the profile line. **Right:** the profile line data with the highest correlation (blue) is plotted with the measurement area data (red) to demonstrate the improved noise reduction.

CONCLUSIONS

Rotary kilns are essential unit operations in many industrial processes including kraft pulping where they are often the most energy-intensive operation in the process. Thermal imaging technology is increasingly being adopted by industry to provide real-time shell temperature measurements and raise alarms when temperatures become too high. In this work we describe several other use-cases for shell temperature data to acquire valuable insights into rotary kiln operation. One such use-case is furthering the industrial understanding of ring formation which is considered one of the most troublesome problems for lime kiln operation. Unfortunately, the widespread lack of appreciation for the potential value in the real-time shell temperature data has contributed to poor data utilization and management. This is exhibited by the inability of existing shell temperature visualization techniques to conveniently and intuitively visualize large quantities of shell temperature data. The work presented in this paper addresses this situation by describing an interactive shell temperature visualization method that is complemented by traditional process analytics to improve kiln monitoring and investigation of abnormal operation. Finally, an industrial case study demonstrates how the proposed KST visualization method led to the detection of rotational aliasing which was resolved with enhanced measurement and processing of shell temperatures.

ACKNOWLEDGEMENTS

The authors thank Spartan Controls, the National Science and Engineering Research Council of Canada, and the Izaak Walton Killam Memorial Fund for funding this research.

REFERENCES

1. Gürtürk, M. and Oztop, H.F., 2014. Energy and exergy analysis of a rotary kiln used for plaster production. Applied thermal engineering, 67(1-2), pp.554-565.

2. Hirtz, B., Marshman, D. and Sheehan, C., 2017. Kiln Infra-Red Cameras for Abnormal Situation Detection and Residual Carbonate Control. JFOR: J. Sci. Technol. For. Prod. Process, 6(3), pp.28-36.

3. Danila, A. and Tamas, F.L., 2020, March. The thermal field analysis of the rotary kiln for the cement plants by means of the image processing techniques. In IOP Conference Series: Materials Science and Engineering (Vol. 789, No. 1, p. 012016). IOP Publishing.

4. Tran, H., 2007. Lime kiln chemistry and effects on kiln operations. Pulp & Paper Centre and Department of Chemical Engineering and Applied Chemistry, University of Toronto, Toronto, Canada.

5. Dernegård, H., Brelid, H. and Theliander, H., 2017. Characterization of a dusting lime kiln–A mill study. Nordic Pulp and Paper Research Journal, 32(1), pp.25-34.

6. Smook, G.A. and Kocurek, M.J., 1982. Handbook for pulp & paper technologists. Canadian Pulp and Paper Association.

7. Järvensivu, M., Juuso, E. and Ahava, O., 2001. Intelligent control of a rotary kiln fired with producer gas generated from biomass. Engineering Applications of Artificial Intelligence, 14(5), pp.629-653.

8. Robinson, J. and Douglas, R., 2011. Improve Lime Mud Kiln Operation by Accurately Sensing and Controlling Mud Moisture. In TAPPI PEERS Conference. TAPPI Press.

9. Rippon, L., Hirtz, B., Sheehan, C., Reinheimer, T., Loewen, P. and Gopaluni, B., 2021. Visualization of multiscale ring formation in a rotary kiln. Nordic Pulp & Paper Research Journal, (0), p.000010151520210048.

10. Adams, T., 1996. Lime kiln principles and operations. In: Proceedings of TAPPI Kraft Recovery Short Course, pp. 2.3.1–18.

11. Le Guen, L. and Huchet, F., 2020. Thermal imaging as a tool for process modelling: application to a flight rotary kiln. Quantitative InfraRed Thermography Journal, 17(2), pp.79-95.

12. Yi, Z., Xiao, H. and Song, J., 2013. An alumina rotary kiln monitoring system based on infrared ray scanning. Measurement, 46(7), pp.2051-2055.

13. Gorog, J.P. and Leary, W., 2016. Ring removal in rotary kilns used by the pulp and paper industry. TAPPI JOURNAL, 15(3), pp.205-213.

14. Mohanan, G., 2017. An Experimental Study on the Effect of Rings on Flame Length and Stability in Lime Kilns (Doctoral dissertation, University of Toronto (Canada)).

15. Tran, H., Mao, X. and Barham, D., 1993. Mechanisms of ring formation in lime kilns. Journal of pulp and paper science, 19(4), p.J167.

16. Keim, E., Zuniga, J. and Tran, H., 2020. Combatting lime kiln ringing problems at the Arauco Constitucion mill. TAPPI JOURNAL, 19(7), pp.345-354.

17. Sun, W. and Braatz, R.D., 2021. Smart process analytics for predictive modeling. Computers & Chemical Engineering, 144, p.107134.

18. Cramer, J.S., 2002. The origins of logistic regression. Tinbergen Institute Discussion Paper, 2002(119/4).

19. Robinson, K., 2019. Optimizing Mill Effectiveness Through Statistical Process Control (SPC). In TAPPI PEERS Conference. TAPPI Press.

20. Rippon, L. 2020. Lime kiln visualization tutorial. https://github.com/LeeRippon/KilnVisual

21. Shannon, C.E., 1949. Communication in the presence of noise. Proceedings of the IRE, 37(1), pp.10-21.

22. Rippon, L.D., Lu, Q., Forbes, M.G., Gopaluni, R.B., Loewen, P.D. and Backström, J.U., 2019. Machine Direction Adaptive Control on a Paper Machine. Industrial & Engineering Chemistry Research, 58(26), pp.11452-11473.